

Zero-biased solar-blind photodetector based on ZnBeMgO/Si heterojunction

This article has been downloaded from IOPscience. Please scroll down to see the full text article.

2009 J. Phys. D: Appl. Phys. 42 152002

(<http://iopscience.iop.org/0022-3727/42/15/152002>)

View [the table of contents for this issue](#), or go to the [journal homepage](#) for more

Download details:

IP Address: 38.107.179.210

The article was downloaded on 22/02/2012 at 11:10

Please note that [terms and conditions apply](#).

FAST TRACK COMMUNICATION

Zero-biased solar-blind photodetector based on ZnBeMgO/Si heterojunction

C Yang^{1,2}, X M Li^{1,3}, W D Yu¹, X D Gao¹, X Cao^{1,2} and Y Z Li^{1,2}¹ State Key Laboratory of High Performance Ceramics and Superfine Microstructures, Shanghai Institute of Ceramics, Chinese Academy of Science, Shanghai 200050, People's Republic of China² Graduate School of Chinese Academy of Science, Beijing 100039, People's Republic of ChinaE-mail: lixm@mail.sic.ac.cn

Received 19 May 2009, in final form 17 June 2009

Published 7 July 2009

Online at stacks.iop.org/JPhysD/42/152002

Abstract

An n-type $\text{Zn}_{1-x-y}\text{Be}_x\text{Mg}_y\text{O}$ thin film was deposited on a p-type Si substrate by pulsed laser deposition to obtain a solar-blind photodetector. The spectral response characteristic with a cutoff wavelength of 280 nm was demonstrated to realize the photodetection of the solar-blind wave zone. The responsivity of the device was improved by inserting an Al-doped ZnO (AZO) contact layer, which was expected to enhance the carrier collection efficiency significantly. Correspondingly, the peak responsivity was improved from 0.003 to 0.11 A W^{-1} at zero bias, and a high external quantum efficiency of 53% at 270 nm was achieved. The fast rise time reached 20 ns. This work demonstrated the possibility of a wurtzite ZnO based oxide system to realize high performance zero-biased solar-blind photodetectors.

1. Introduction

The solar-blind ultraviolet (UV) photodetector possesses vast potential applications in the fields of solar astronomy, missile plume detection, space-to-space transmission, fire alarms and combustion monitoring [1–3], since its operating spectrum range (220–280 nm) avoids interference from solar radiation [1].

As the most promising candidate for UV detectors, wurtzite ZnO has attracted considerable interest in recent years due to its high bandgap energy (3.4 eV), radiation hardness, high temperature resistance, low growth cost and vast possibility to modulate its bandgap through doping techniques [4, 5].

For the solar-blind UV detector, its cutoff working wavelength should be lower than 280 nm, corresponding to the bandgap wider than 4.4 eV. In recent years, the bandgap modulation of ZnO films by alloying with a wider bandgap semiconductor MgO (7.8 eV) has been widely investigated [6–10]. However, a wide miscibility gap exists in the ZnO–MgO binary system due to the structure difference and

large lattice mismatch between ZnO (wurtzite, 3.25 Å) and MgO (rock salt, 4.22 Å) [6]. Therefore, the phase segregation has become the key problem of MgZnO bandgap modulation between 4.2 and 5.4 eV [7]. Recently, nonequilibrium growth processes and structural coherency with a compatible substrate were utilized to grow metastable cubic MgZnO films for solar-blind detection [11, 12]. But there is still no stable single-phased wurtzite MgZnO film obtained with bandgap modulated within the solar-blind region up to now. Hence, another binary system $\text{Be}_x\text{Zn}_{1-x}\text{O}$ was proposed [13, 14], since BeO has the same hexagonal wurtzite structure with ZnO and a much wider bandgap of 10.8 eV. But the large ionic radius difference between Be^{2+} (0.27 Å) and Zn^{2+} (0.60 Å) will generate noticeable lattice mismatch when large bandgap offset between BeZnO and ZnO is wanted [15]. In our previous study, the single-phased wurtzite ZnO based oxide system $\text{Zn}_{1-x-y}\text{Be}_x\text{Mg}_y\text{O}$ had been successfully prepared with bandgap continuously modulated from 3.7 to 4.9 eV, and the advantage of crystalline and optical properties had been demonstrated compared with those of ZnMgO and BeZnO [16].

Considering the difficulty of achieving stable and reproducible high-quality p-type ZnO layers, many studies

³ Author to whom any correspondence should be addressed.

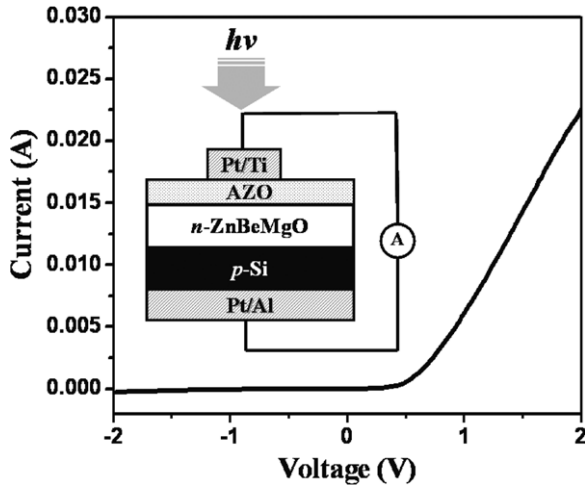


Figure 1. I - V characteristic of the n-ZnBeMgO/p-Si heterojunction. The inset is the schematic cross-section of the device.

have been reported on the n-ZnO/p-Si heterojunction photodiodes [17, 18] for compatibility with Si integrated circuit (IC) technology. However, high performance solar-blind ZnO based photodetectors have not yet been obtained. Moreover, an external (reverse) bias is required to achieve high photoresponsivity for most ZnO/Si photodiodes, and high photoresponsivity ZnO/Si photodiodes without bias are seldom reported [18].

In this paper, the solar-blind photodetector based on a $Zn_{1-x-y}Be_xMg_yO$ system without bias is demonstrated. As a device structure of photodiode, n-type single-phased wurtzite ZnBeMgO films were deposited on p-type Si substrates to form a heterojunction. The spectral and temporal response characteristics of the devices were studied. Meanwhile, for the purpose of obtaining a high-quality ohmic contact between the metal electrode and the high resistivity ZnBeMgO layer, an AZO contact layer was introduced for comparison.

2. Experimental details

ZnBeMgO films were deposited on p-Si and quartz substrates by pulsed laser deposition at a substrate temperature of 600 °C. The oxygen partial pressure was 1×10^{-4} Pa. Ceramic $Zn_{0.7}Be_{0.1}Mg_{0.2}O$ targets were ablated by a KrF excimer laser (Lambda Physik COMPex, wavelength of 248 nm, energy of 200 mJ pulse⁻¹ and a repetition rate of 5 Hz). The thickness of the deposited films was about 300 nm. To analyse the spectral response properties of the ZnBeMgO/Si heterojunction, ohmic contacts were made by depositing a regular semi-transparent Ti/Pt electrode on n-ZnBeMgO and an Al/Pt electrode on the reverse of p-Si [17]. Furthermore, in order to reduce the specific contact resistance between the metal electrode and the ZnBeMgO layer, an additional highly doped $Zn_{0.98}Al_{0.02}O$ (AZO) thin film (thickness of ~50 nm, sheet resistance of ~70 Ω/□) was introduced as a contact layer for comparison.

The device structure is illustrated in the inset of figure 1, and operating without bias. The spectral response was carried out using a 150 W Xe arc lamp and a monochromator.

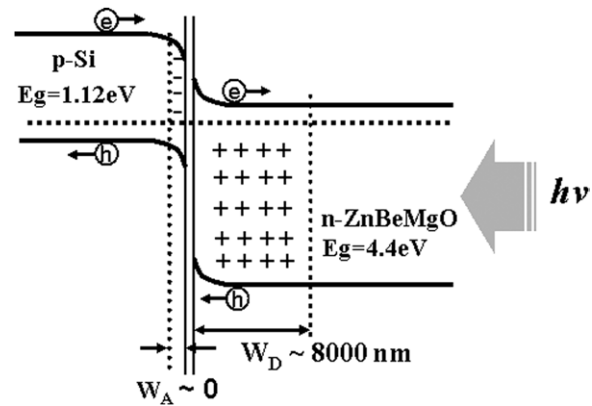


Figure 2. The schematic band structure of the n-ZnBeMgO/p-Si heterojunction.

A chopper was used to chop light before casting it on the sample. The generated photocurrent was fed to the lock-in amplifier. The incident power on the sample was calibrated using a commercial UV enhanced Si photodiode, from which the responsivity values were obtained. The pulsed KrF laser (248 nm) was used to measure the time response as the excitation source.

3. Results and discussion

Electrical properties were measured at room temperature by Hall measurements with the Van der Pauw configuration. Figure 1 displays the rectifying character of the n-ZnBeMgO/p-Si heterojunction, with the threshold voltage of ~0.5 V. The dark current of the diodes was approximately 10^{-6} A at 5 V bias, which is three orders of magnitude higher than that of GaN-based solar-blind detectors. This high dark current was mainly due to the defects in films and interfaces, and could be further decreased by improving the crystalline quality of ZnBeMgO films.

According to the Anderson model as shown in figure 2, the depletion width in p-Si (W_A) and in n-ZnO (W_D) was inversely proportional to their carrier concentrations [19]

$$\frac{W_A}{W_D} = \frac{N_D}{N_A}, \quad (1)$$

where N_A is the acceptor concentration of p-Si ($\sim 10^{18}$ cm⁻³) and N_D is the donor concentration of n-ZnBeMgO ($\sim 10^{13}$ cm⁻³). Therefore, the estimated ratio of depletion width in p-Si to n-ZnBeMgO is below 10^{-5} , and the heterojunction can be approximated to a one-sided junction. Hence, the visible light responsivity generated in the depleted p-Si layer is eliminated. The calculated depletion width in the n-ZnBeMgO side is approximately 8000 nm, covering the whole ZnBeMgO film.

The optical properties were characterized by a UV-VIS-NIR (Shimadzu) spectrometer at room temperature. The sharp cutoff and Fabry-Perot oscillations of the transmission spectra for an individual ZnBeMgO layer, shown in figure 3, confirm the high quality of the film. Solar blindness is guaranteed by the cutoff wavelength of 280 nm.

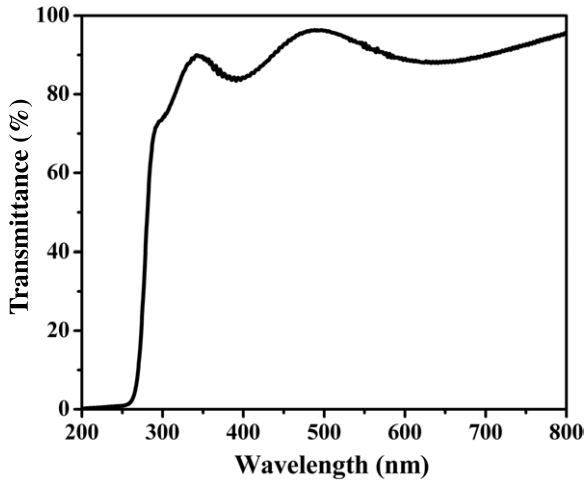


Figure 3. Transmittance spectra of an individual ZnBeMgO layer.

The absolute spectral responsivity of the n-ZnBeMgO/p-Si heterojunction photodiode without bias is plotted in figure 4. The response curves drop two orders of magnitude by 280 nm and remain at low response for the entire near UV and visible spectrum, demonstrating a typical solar-blind photoelectric response characteristic. However, due to the high resistivity of the ZnBeMgO layer and the weak UV output from the light source, the collection of photogenerated carriers is less efficient without a contact layer [20].

In order to enhance the carrier collection efficiency, an additional AZO film was deposited on ZnBeMgO as a highly doped contact layer. The conductive mechanism could be explained as follows. For a metal–semiconductor contact with a low semiconductor doping concentration ($\sim 10^{13} \text{ cm}^{-3}$ for ZnBeMgO), the thermionic emission current is dominant in this junction, and the specific contact resistance for this case decreases rapidly as the barrier height decreases. For the metal–semiconductor junction with a high impurity doping concentration ($> 10^{21} \text{ cm}^{-3}$ for AZO), the tunnelling process will dominate. Thus the specific contact resistance is a very strong function of semiconductor doping. Therefore, a heavily doped AZO layer was designed at the surface in our device as an ohmic contact layer. There is a tradeoff, however, between the improvement in carrier collection and the reduction of photons arriving at the ZnBeMgO layer due to the absorption in the AZO layer.

As a result, the peak responsivity improved significantly from 0.003 to 0.11 A W^{-1} at 270 nm without bias, as shown in figure 4, despite the weak response attributed to the AZO layer ($E_g \sim 3.4 \text{ eV}$) observed around 360 nm . This responsivity is much higher than that of cubic MgZnO solar-blind photodetectors (0.1 mA W^{-1} under 10 V bias). The theoretical current responsivity for a photodiode is given by [21]

$$R(\lambda) = \frac{q\lambda}{hc} \eta, \quad (2)$$

where λ is the photon wavelength and η is the external quantum efficiency (QE). As shown in the inset of figure 4, the external QE reaches as high as 53% at 270 nm without bias, which is comparable to that of GaN photodiodes [2, 20–22].

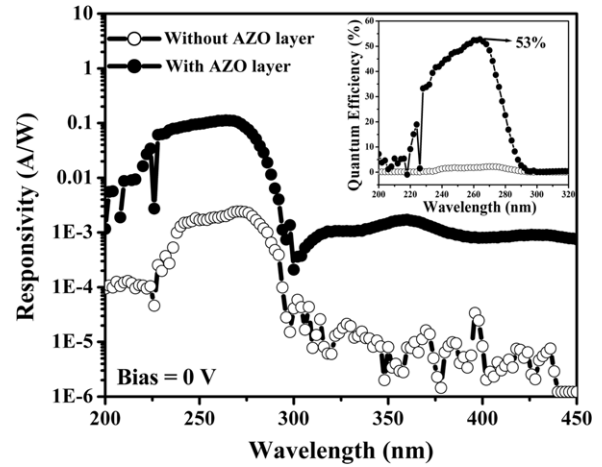


Figure 4. Measured spectral responsivity curves at zero bias of the n-ZnBeMgO/p-Si heterojunction. The inset is the corresponding external quantum efficiency of the device.

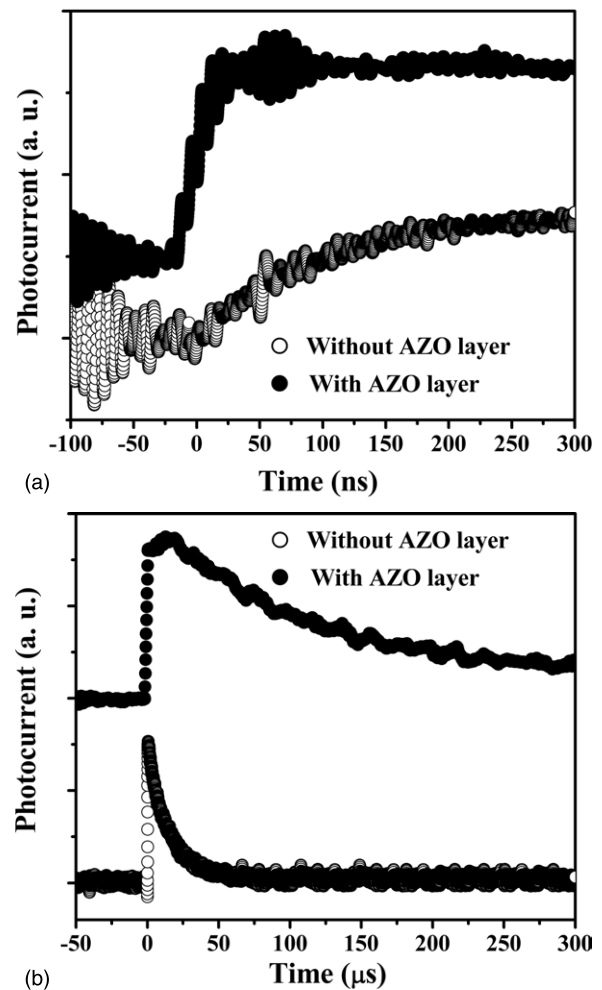


Figure 5. Temporal response (a) rise and (b) fall edge with a pulsed KrF laser as the optical source.

The 10–90% response time of the heterojunction photodiode is shown in figure 5. The rise time dramatically shortened from 200 to 20 ns when AZO contact layer was utilized. This could be attributed to the change in the dominant conductive mechanism from thermionic emission current to

tunnelling current. The 20 ns rise time is limited mainly by the excitation laser pulse width of 10 ns. It was much faster than that of most ZnO based photodetectors reported [23]. However, the fall time of the photodiode delayed for 30 μ s, and increased to 250 μ s by introducing the AZO layer. It was related to the trapping of photogenerated carriers by the defects in films and interfaces [23, 24]. The AZO layer was deposited at room temperature, revealing much more structure defects than ZnBeMgO. That is, the fall time could be potentially shortened by preparing the contact layer with higher crystalline quality.

4. Conclusions

In conclusion, zero-biased solar-blind photodetectors based on the n-Zn_{1-x-y}Be_xMg_yO/p-Si heterojunction with a cutoff wavelength of 280 nm were fabricated by the pulsed laser deposition method. The responsivity of the device was 0.003 A W⁻¹ at zero bias with a UV/visible rejection ratio of more than two orders of magnitude. Further improvement in responsivity was achieved by enhancing the carrier collection efficiency using a thin Al-doped ZnO contact layer, and the peak responsivity significantly improved to 0.11 A W⁻¹ at zero bias, corresponding to a high external quantum efficiency of 53%. The rise time achieved was as fast as 20 ns. Although the fall time was 250 μ s, it could be potentially shortened by preparing the contact layer with higher crystalline quality. This work demonstrates the possibility of a wurtzite ZnO based oxide system in realizing high performance zero-biased photodetector with a typical solar-blind photoelectric response characteristic.

Acknowledgments

This work was sponsored by the Shanghai-AM Research and Development Fund (08700740900) and the Nature Science Foundation of Shanghai (08ZR1421500).

References

- [1] Walker D, Kumar V, Mi K, Sandvik P, Kung P, Zhang X H and Razeghi M 2000 *Appl. Phys. Lett.* **76** 403
- [2] Tut T, Yelboga T, Ulker E and Ozbay E 2008 *Appl. Phys. Lett.* **92** 103502
- [3] Soltani A, Zhang W J and BenMoussa A 2008 *Appl. Phys. Lett.* **92** 053501
- [4] Service R F 1997 *Science* **276** 5314
- [5] Özgür Ü, Alivov Ya I, Liu C, Teke A, Reshchikov M A, Dogan S, Avrutin V, Cho S-J and Morkoç H 2005 *J. Appl. Phys.* **98** 041301
- [6] Ohtomo A, Kawasaki M, Koida T, Masubuchi K, Koinuma H, Sakurai Y, Yoshida Y, Yasuda T and Segawa Y 1998 *Appl. Phys. Lett.* **72** 2466
- [7] Takeuchi I, Yang W, Chang K-S, Aronova M A, Venkatesan T, Vispute R D and Bendersky L A 2003 *J. Appl. Phys.* **94** 7336
- [8] Hullavarad S S, Dhar S, Varughese B, Takeuchi I and Venkatesan T 2005 *J. Vac. Sci. Technol. A* **23** 982
- [9] Zhang X, Li X M, Chen T L, Zhang C Y and Yu W D 2005 *Appl. Phys. Lett.* **87** 092101
- [10] Kong J F, Shen W Z, Zhang Y W, Yang C and Li X M 2008 *Appl. Phys. Lett.* **92** 191910
- [11] Yang W, Hullavarad S S, Nagaraj B, Takeuchi I, Sharma R P, Venkatesan T, Vispute R D and Shen H 2003 *Appl. Phys. Lett.* **82** 3424
- [12] Ju Z G, Shan C X, Jiang D Y, Zhang J Y, Yao B, Zhao D X, Shen D Z and Fan X W 2008 *Appl. Phys. Lett.* **93** 173505
- [13] Ryu Y R, Lee T S, Lubguban J A, Corman A B, White H W, Leem J H, Han M S, Park Y S, Youn C J and Kim W J 2006 *Appl. Phys. Lett.* **88** 052103
- [14] Kim W J, Leem J H, Han M S, Park I-W, Ryu Y R and Lee T S 2006 *Appl. Phys. Lett.* **99** 096104
- [15] Ding S F, Fan G H, Li S T, Chen K and Xiao B 2007 *Physica B* **394** 127
- [16] Yang C, Li X M, Gu Y F, Yu W D, Gao X D and Zhang Y W 2008 *Appl. Phys. Lett.* **93** 112114
- [17] Gu Y F, Li X M, Zhao J L, Yu W D, Gao X D and Yang C 2007 *Solid State Commun.* **143** 421
- [18] Huang H, Fang G, Mo X, Yuan L, Zhou H, Wang M, Xiao H and Zhao X 2009 *Appl. Phys. Lett.* **94** 063512
- [19] Sze S M 1981 *Physics of Semiconductor Devices* 2nd edn (New York: Wiley) 124pp
- [20] Biyikli N, Aytur O, Kimukin I, Tut T and Ozbay E 2002 *Appl. Phys. Lett.* **81** 3272
- [21] Walker D, Saxler A, Kung P, Zhang X, Hamilton M, Diaz J and Razeghi M 1998 *Appl. Phys. Lett.* **72** 3303
- [22] Collins C J, Li T, Lambert D J H, Wong M M, Dupuis R D and Campbell J C 2000 *Appl. Phys. Lett.* **77** 2810
- [23] Jiang D, Zhang J, Lu Y, Liu K, Zhao D, Zhang Z, Shen D and Fan X 2008 *Solid-State Electron.* **52** 679
- [24] Liang S, Sheng H, Liu Y, Huo Z and Lu Y 2001 *J. Cryst. Growth* **225** 110